Fullerometallic Ion Chemistry: Reactions of $C_{60}Fe^+$ and $C_{20}H_{10}Fe^+$ in the Gas Phase

Doina Caraiman,[†] Gregory K. Koyanagi,[†] Lawrence T. Scott,[‡] Dorin V. Preda,[‡] and Diethard K. Bohme*,[†]

Contribution from the Department of Chemistry, Centre for Research in Mass Spectrometry, and Centre for Research in Earth and Space Science, York University, Toronto, Ontario M3J 1P3, Canada, and Department of Chemistry, Merkert Chemistry Center, Boston College, Chestnut Hill, Massachusetts 02467-3860

Received February 22, 2001

Abstract: Fe^+ has been attached to buckminsterfullerene, C_{60}, and corannulene, $C_{20}H_{10}$, in the gas phase, and the reactivities of $C_{60}Fe^+$ and $C_{20}H_{10}Fe^+$ have been measured with several small inorganic and organic molecules in helium bath gas at 0.35 Torr using a selected-ion flow tube (SIFT) mass spectrometer. Comparisons with measured reactivities of the bare Fe^+ ion indicate that the presence of C_{60} and $C_{20}H_{10}$ leads to enhancements in reactivity at room temperature of up to 5 orders of magnitude. Ligation was the only chemistry observed with D_2, N_2, CO_2, CH_4, C_2H_2, C_2H_4, SO_2, C_6D_6, NH_3, H_2O, and CO, but other channels were observed to compete with adduct formation in the reactions with N_2O and O_2. The number of molecules sequentially ligated to the ion was different: up to five molecules of ligand added sequentially to Fe^+, up to four molecules of ligand were observed to attach to $C_{60}Fe^+$, while only up to three molecules added to $C_{20}H_{10}Fe^+$. C_{60}^+ and $C_{20}H_{10}^+$ were observed to be unreactive toward the same ligands. The kinetic results show the influence of carbonaceous surfaces on metal ion reactivity and are interpreted in terms of the nature of the coordination of Fe^+ to the carbonaceous surface. Catalytic effects of the carbonaceous surfaces were identified for the reactions with N_2O and O_2.

Introduction

The study of fullerometallic chemistry began with the pioneering work of Smalley and co-workers, who observed the formation of the endohedral La@C_{60} species in laser vaporization studies.[1] Since then, several research groups have explored exohedral and endohedral metallofullerenes and their ionic counterparts in the gas phase,[2a,d] in the condensed phase[3a,e] and from a theoretical point of view.[4a,c] Huang and Freiser generated exohedral $C_{60}M^+$ species (M = Fe, Co, Ni, Cu, Rh, La, V) in an ICR−FTMS mass spectrometer via a multistep sequence initiated by laser desorption to generate M^+ from pure metal targets followed by the reaction of the metal ion with C_{60}.[5] For metal ions that reacted with C_{60} predominantly by electron transfer, a procedure involving ligand exchange was used in order to enhance the $C_{60}M^+$ intensity over that observed by direct attachment. Low-energy collision-induced dissociation (CID) experiments with $C_{60}M^+$ in Ar buffer gas (at about 2×10^{-6} Torr) indicated formation of either M^+ or C_{60}^+ depending on IE(M) and a weak interaction between the exohedral metal ion and the carbon surface ($D(C_{60}-Fe^+) = 44 \pm 7$ kcal mol^{-1}).[6] Exohedral $C_{60}M^+$ species (M = Fe, Mn, Cr, Mo, W) have also been obtained in a guided ion beam mass spectrometer from the direct reaction of metal ions generated by electron-bombardment ionization of metal carbonyls and C_{60} vapor.[7] Two distinct types of $C_{60}Fe^+$ complexes were observed to be formed over a collision energy range from 1 to 100 eV. At low collision energies, a weakly bound (coordination) complex was formed with no activation barrier that dissociates by loss of Fe. A second type of $C_{60}Fe^+$ complex was observed at collision energies above 10 eV. This high-energy complex has a substantial activation barrier to formation, is chemically bound, and decomposes by loss of metal dicarbide (FeC_2) or Fe. A network structure has been proposed for this complex, with the metal probably sitting above the fullerene surface, chemically bound to two or more carbon atoms.

Here we investigate the gas-phase reactivity of $C_{60}Fe^+$ and $C_{20}H_{10}Fe^+$ using the selected-ion flow tube technique with a

[†] York University.
[‡] Boston College.

(1) Heath, J. R.; O'Brien, S. C.; Zhang, Q.; Liu, Y.; Curl, R. F.; Kroto, H. W.; Tittel, F. K.; Smalley, R. E. *J. Am. Chem. Soc.* **1985**, *107*, 7779−7780.

(2) (a) Roth, L. M.; Huang, Y.; Schwedler, J. T.; Cassady, C. J.; Ben-Amotz, D.; Kahr, B.; Freiser, B. S. *J. Am. Chem. Soc.* **1991**, *113*, 6299−6300. (b) Zimmerman, P.; Hercules, D. M. *Appl. Spectrosc.* **1993**, *47* (10), 1545−1547. (c) Basir, Y.; Wan, Z.; Christian, J. F.; Anderson, S. L. *Int. J. Mass Spectrom. Ion Processes* **1994**, *138*, 173−185. (d) Kurikawa, T.; Nagao, S.; Miyajima, K.; Nakajima, A.; Kaja, K. *J. Phys. Chem.* **1998**, *102*, 1743−1747.

(3) (a) Fagan, P. J.; Calabrese, J. C.; Malone, B. *Acc. Chem. Res.* **1992**, *25*, 134−142. (b) Pradeep, T.; Kulkarni, G. U.; Kannan, K. R.; Guru Row: T. N.; Rao, C. N. R. *J. Am. Chem. Soc.* **1992**, *114*, 2272−2273. (c) Douthwaite, R. E.; Green, M. L. H.; Stephens, A. H. H.; Turner F. C. *J. Chem. Soc., Chem. Commun.* **1993**, 1522−1523. (d) Rasinkangas, M.; Pakkanen, T.; Pakkanen, T. A. *J. Organomet. Chem.* **1994**, *476*, C6−C8. (e) Sueki, K.; Kikuchi, K.; Akiyama, K.; Sawa, T.; Katada, M.; Ambe, F.; Nakahara, H. *Chem. Phys. Lett.* **1999**, *300*, 140−144.

(4) (a) Rogers, J. R.; Marynick, D. S. *Chem. Phys. Lett.* **1993**, *205* (2, 3), 197−199. (b) Fujimoto, H.; Nakao, Y.; Kukui, K. *J. Mol. Struct.* **1993**, *300*, 425−434. (c) Lopez, J. A.; Mealli, C. *J. Organomet. Chem.* **1994**, *478*, 161−171.

(5) Huang, Y.; Freiser, B. S. *J. Am. Chem. Soc.* **1991**, *113*, 9418−9419.

(6) Kan, S.; Byun, Y. G.; Lee, S. A.; Freiser, B. S. *J. Mass Spectrom.* **1995**, *30*, 194−200.

(7) Basir, Y. J.; Anderson, S. L. *Int. J. Mass Spectrom.* **1999**, *185/186/187*, 603−615.

10.1021/ja0104857 CCC: $20.00
Published on Web 08/11/2001

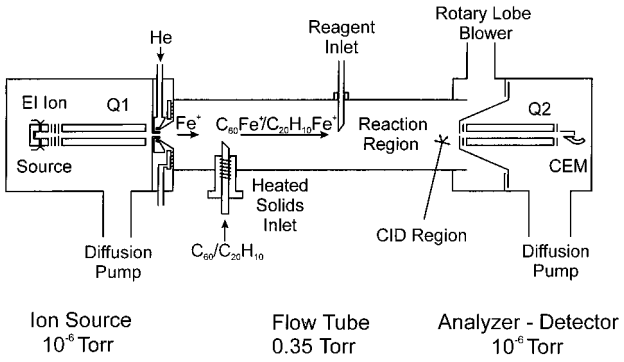

Figure 1. EI/SIFT apparatus adapted for the generation of fullerometallic ions and for kinetic studies of ion−molecule reactions.

range of small organic and inorganic molecules. Corannulene, $C_{20}H_{10}$ (dibenzo[*ghi*,*mno*]fluoranthene), with its highly strained bowl-like structure, has a carbon skeleton that appears at every five-membered ring on the surface of C_{60} and other fullerenes. Both metal ion−carbonaceous surface complexes have been generated in our instrument by the direct association reaction of Fe^+ with neutral C_{60} or corannulene vapor. We extend here our early studies[8] on $C_{60}Fe^+$ and report, for the first time, the formation and chemistry of the complex ions $C_{20}H_{10}Fe^+$ and $(C_{20}H_{10})_2Fe^+$. Reactions are investigated with D_2, N_2, CH_4, CO_2, SO_2, C_2H_4, C_2H_2, H_2O, NH_3, CO, N_2O, O_2, and C_6D_6. Both rate coefficients and product ion distributions have been measured, and these, when compared to similar measurements with the bare Fe^+ ion, provide insight into fundamental aspects of the influence of a carbonaceous surface on metal ion chemistry, including possible catalytic effects. They also provide insight into the mode of coordination between the metal ion and the fullerene/corannulene substrate.

The gas-phase experiments reported here provide a probe of the intrinsic features of Fe^+ coordination with corannulene and C_{60} in the absence of complicating factors that may arise in the condensed phase due to solvation or ion pairing. Consequently, they can serve as a benchmark for the chemistry of fullerometallic cations in solution.

Experimental Section

The kinetic results reported here were obtained using the selected-ion flow tube (SIFT) apparatus (see Figure 1). The experimental setup and operating conditions for the SIFT apparatus have been described in detail previously.[9] All measurements were performed in a helium buffer gas with a pressure of 0.35 ± 0.01 Torr. The reactant Fe^+ was generated from pure ferrocene, $(c\text{-}C_5H_5)_2Fe$, vapor in a low-pressure ionization source by 70 eV electron-impact dissociative ionization. The metal ions were mass selected with the quadrupole mass filter and injected in the flow tube containing He buffer gas. The fullerene/corannulene adducts were obtained upstream in the flow tube by adding neutral C_{60}/corannulene from heated samples. Minor electron-transfer channels also afforded C_{60}^+ and $C_{20}H_{10}^+$, respectively. The ions were thermalized by collisions with He buffer gas (about 10^5 collisions) before entering the reaction region downstream in the flow tube where the neutral reagents were added. Reactant and product ions were monitored still farther downstream with a second quadrupole mass filter as a function of the neutral reagent flow.

Rate coefficients for the primary reactions of all ions present in the system are determined with an uncertainty estimated to be less than ±30% from the rate of decay of the reactant ion intensity. Rate coefficients for secondary and higher-order reactions can be obtained by fitting the experimental data to solutions of differential equations for chains of successive reactions.

Previous studies by Viggiano et al. have shown that weakly ligated clusters (with binding energies lower than 13 kcal mol^{-1}) can undergo thermal dissociation in high-pressure flow tube instruments.[10a] In our instrument, weak ligation can also be discriminated against in the sampling process due to collisional dissociation resulting from the presence of a small electric field at the nose cone that is biased at ca. −7 V. Previous experience in our laboratory indicates that ligand binding energies must be at least 10 kcal mol^{-1} for the ligated species to survive thermal dissociation or dissociation upon sampling.[10b]

The multicollision-induced dissociation (CID) of sampled ions is investigated by raising the potential of the sampling nose cone from −4 to −80 V. Thresholds for dissociation are obtained from plots of relative ion intensities as a function of accelerating voltage, and these provide information on bond connectivities.[11]

The C_{60} samples used in this work were purchased from SES Research and were 99.5+%, reagent grade, while the corannulene samples were synthesized at Boston College according to a three-step synthesis detailed elsewhere.[12]

Reactant neutrals were introduced into the reaction region either as a pure gas (N_2), as a mixture in helium, or as vapors diluted in helium to various levels (H_2O and C_6D_6). All neutrals (except for deionized water) were obtained commercially and were of high purity (>99.5%); the neutral reagents were used without further purification, except for the liquid compounds that were subjected to multiple freeze−pump−thaw cycles to remove noncondensable gases.

Results and Discussion

Production of $C_{60}Fe^+$ and $C_{20}H_{10}Fe^+$. $C_{60}Fe^+$ was produced by the association reaction of Fe^+ with C_{60} upstream of the reaction region (see Figure 1). The C_{60} vapor was obtained from a fullerene sample heated to about 500 °C in a stainless steel shielded inlet and was introduced into the flow tube upstream of the reaction region. A temperature gradient of approximately 50 °C was measured with a thermocouple along the outside wall and inside along the axis of the SIFT from the position of the inlet containing the C_{60} oven to the position of the entrance of the reaction region. But the temperature within the reaction region was essentially constant at 298 K. The solid probe inlet did not allow significant variation or accurate measurement of the C_{60} vapor flow and so prevented the determination of the rate coefficient for the reaction between Fe^+ and C_{60}. Instead, the C_{60} flow, and therefore the upstream concentration of $C_{60}Fe^+$, was held constant by heating the fullerene sample at a constant temperature during all experiments. The flow of C_{60} vapor was estimated using the electron-transfer reaction between Ar^+ and C_{60} and assuming that electron transfer occurs on every collision, $k_c = 3.5 \times 10^{-9}$ cm^3 $molecule^{-1}$ s^{-1} (calculated using the algorithm of the combined variational transition-state theory developed by Su and Chesnavich[13]). The change in the Ar^+ ion intensity upon the addition of C_{60} then provided a C_{60} flow of about 2×10^{15} molecules s^{-1}. The rate coefficient for the reaction between Fe^+ and C_{60} could in turn be estimated to be 7×10^{-10} cm^3 $molecule^{-1}$ s^{-1}, which is approximately 20% of the collision rate coefficient, $k = 3 \times 10^{-9}$ cm^3 $molecule^{-1}$ s^{-1}. Fe^+ was observed to react with C_{60} by association to produce $C_{60}Fe^+$ and by electron transfer to produce C_{60}^+ in a ratio of about 5:1 according to reaction 1.

(8) Baranov, V.; Bohme, D. K. *Int. J. Mass Spectrom. Ion Processes* **1995**, *149/150*, 543−553.

(9) Mackay, G. I.; Vlachos, G. D.; Bohme, D. K.; Schiff, H. I. *Int. J. Mass Spectrom. Ion Phys.* **1980**, *36*, 259−270.

(10) (a) Hierl, P. M.; Ahrens, A. F.; Henchman, M. J.; Viggiano, A. A.; Paulson, J. F. *Int. J. Mass Spectrom. Ion Processes* **1987**, *81*, 101. (b) Milburn, R. K.; Baranov, V. I.; Hopkinson, A. C.; Bohme, D. K. *J. Phys. Chem. A* **1998**, *102*, 9803−9810.

(11) Baranov, V.; Bohme, D. K. *Int. J. Mass Spectrom. Ion Processes* **1996**, *154*, 71−88.

(12) Scott, L. T.; Cheng, P. C.; Hashemi, M. M.; Bratcher, M. S.; Meyer, D. T.; Warren, H. B. *J. Am. Chem. Soc.* **1997**, *119*, 10963−10968.

(13) Su, T.; Chesnavich, J. *J. Chem. Phys.* **1982**, *76*, 5183−5185.

Table 1. Reaction Rate Coefficients (k_{obs} in cm^3 $molecule^{-1}$ s^{-1}) Measured for the Primary Reactions and Collision Rate Coefficients (k_{cap} in cm^3 $molecule^{-1}$ s^{-1}) Calculated Using the Algorithm of a Modified Variational Transition Sate Theory[13] for Fe^+, C_{60}^+, $C_{60}Fe^+$, $C_{20}H_{10}^+$, and $C_{20}H_{10}Fe^+$ Reacting with Selected Organic and Inorganic Molecules in He at 0.35 Torr and 298 K

	k_{obs} [k_{cap}]				
ligand	Fe^+	C_{60}^+	$C_{60}Fe^+$	$C_{20}H_{10}^+$	$C_{20}H_{10}Fe^+$
D_2	$<10^{-13}$ [1.4×10^{-9}]	$<10^{-12}$ [1.4×10^{-9}]	$>6.3 \times 10^{-12}$ [1.4×10^{-9}]	$<10^{-12}$ [1.4×10^{-9}]	$>1.6 \times 10^{-11}$ [1.4×10^{-9}]
N_2	$<10^{-14}$ [7.2×10^{-10}]	$<10^{-12}$ [5.9×10^{-10}]	2.6×10^{-10} [5.9×10^{-10}]	$<7 \times 10^{-12}$ [6.1×10^{-10}]	1.5×10^{-10} [6.1×10^{-10}]
CO_2	$<10^{-15}$ [8.0×10^{-10}]	$<10^{-12}$ [6.2×10^{-10}]	3.5×10^{-10} [6.2×10^{-10}]	$<7 \times 10^{-12}$ [6.5×10^{-10}]	$>5.4 \times 10^{-11}$ [6.4×10^{-10}]
CH_4	$<5 \times 10^{-14}$ [1.1×10^{-9}]	$<10^{-12}$ [9.5×10^{-10}]	4.3×10^{-10} [9.5×10^{-10}]	$<9 \times 10^{-13}$ [9.7×10^{-10}]	$>1.3 \times 10^{-10}$ [9.7×10^{-10}]
SO_2	8.1×10^{-12} [1.7×10^{-9}]	$<10^{-13}$ [1.2×10^{-9}]	6.6×10^{-10} [1.2×10^{-9}]	$<10^{-12}$ [1.3×10^{-9}]	7.8×10^{-10} [(1.2×10^{-9}]
C_2H_4	6.1×10^{-11} [1.2×10^{-9}]	$<10^{-12}$ [9.6×10^{-10}]	6.1×10^{-10} [9.6×10^{-10}]	$<5 \times 10^{-12}$ [9.9×10^{-10}]	6.4×10^{-10} [9.8×10^{-10}]
C_2H_2	1.6×10^{-11} [1.0×10^{-9}]	$<10^{-12}$ [8.5×10^{-10}]	4.3×10^{-10} [8.5×10^{-10}]	$<10^{-13}$ [8.8×10^{-10}]	4.7×10^{-10} [8.7×10^{-10}]
H_2O	$<10^{-13}$ [2.4×10^{-9}]	$<10^{-11}$ [2.1×10^{-9}]	4.2×10^{-10} [2.1×10^{-9}]	$<6 \times 10^{-12}$ [2.2×10^{-9}]	4.3×10^{-10} [2.1×10^{-9}]
NH_3	1.7×10^{-11} [2.2×10^{-9}]	$<10^{-12}$ [1.9×10^{-9}]	7.7×10^{-10} [1.9×10^{-9}]	$<6 \times 10^{-13}$ [2×10^{-9}]	7.2×10^{-10} [1.9×10^{-9}]
CO	$<10^{-14}$ [7.8×10^{-10}]	$<10^{-12}$ [6.5×10^{-10}]	3.9×10^{-10} [6.5×10^{-10}]	$<10^{-13}$ [6.7×10^{-10}]	2.5×10^{-10} [6.6×10^{-10}]
C_6D_6	9×10^{-10} [1.3×10^{-9}]	$<10^{-12}$ [8.6×10^{-10}]	8.6×10^{-10} [8.6×10^{-10}]	$<10^{-11}$ [9.5×10^{-10}]	8.4×10^{-10} [9.3×10^{-10}]
N_2O	3.1×10^{-11} [8.5×10^{-10}]	$<10^{-12}$ [6.6×10^{-10}]	5.2×10^{-10} [6.6×10^{-10}]	$<10^{-13}$ [6.9×10^{-10}]	3.8×10^{-10} [6.8×10^{-10}]
O_2	$<10^{-14}$ [6.5×10^{-10}]	$<10^{-12}$ [5.3×10^{-10}]	2.3×10^{-10} [5.3×10^{-10}]	$<10^{-11}$ [5.5×10^{-10}]	2.7×10^{-10} [5.4×10^{-10}]

$$Fe^+ + C_{60} \rightarrow C_{60}Fe^+ \quad (1a)$$

$$\rightarrow Fe + C_{60}^+ \quad (1b)$$

Adduct formation in channel 1a is presumed to occur by termolecular association with He atoms serving as a stabilizing third body. The minor electron-transfer channel 1b is exothermic by approximately 0.3 eV (IE(Fe) = 7.9024 ± 0.0001 eV,[14] IE(C_{60}) = 7.64 ± 0.02 eV [15]). Our results are in contrast to what has been observed by other research groups for the reaction between Fe^+ and C_{60} at low pressures ($<10^{-4}$ Torr),[5,7] in which electron transfer predominates over association. The He buffer gas in our higher-pressure experiments both cools the C_{60} by collisions before it reacts with Fe^+ and stabilizes by collisions the adducts formed with Fe^+.

A similar procedure was used to generate $C_{20}H_{10}Fe^+$ from the direct reaction of Fe^+ with $C_{20}H_{10}$. Fe^+ was generated in the same way, and corannulene was added using the same solid probe inlet but now heated to only about 140 °C. The reaction between Fe^+ and $C_{20}H_{10}$ generates $C_{20}H_{10}Fe^+$ from the association channel and $C_{20}H_{10}^+$ from the electron-transfer channel in a ratio of about 30:1. Electron transfer is even less exothermic than in the case of Fe^+ reacting with C_{60}, IE($C_{20}H_{10}$) = 7.70 ± 0.01 eV.[16] Again, the rate coefficient for the reaction between Fe^+ and corannulene could not be measured. A constant flow of corannulene vapor was maintained in all experiments by heating the sample at constant temperature. A second molecule of $C_{20}H_{10}$ was observed to add to $C_{20}H_{10}Fe^+$ to form $C_{20}H_{10}$-$FeC_{20}H_{10}^+$. Our current mass range capabilities did not allow us to identify a similar adduct for C_{60}, ($C_{60}FeC_{60}^+$), the "dumbell" that has been observed by others with other metal ions.[2d,17,18]

Overview of Primary Reaction Kinetics. Table 1 presents a summary of the measured rate coefficients, k_{obs}, for the primary reaction steps in the reactions of Fe^+, C_{60}^+ and $C_{60}Fe^+$, $C_{20}H_{10}^+$ and $C_{20}H_{10}Fe^+$ with the selected neutral molecules. Also included are collision rate coefficients, k_{cap}, calculated using the variational transition-state theory of Su and Chesnavich.[13] The ratio k_{obs}/k_{cap} provides a measure of reaction probability. Ligation was the main chemistry observed in all of these ion molecule reactions, but other channels were observed to compete with the adduct formation in reactions with N_2O and O_2.

C_{60}^+ was observed to be unreactive toward all the molecules investigated, $k_{obs} < 10^{-12}$ cm^3 $molecule^{-1}$ s^{-1}, in agreement with previous studies that have shown that monocations of C_{60} are generally unreactive under SIFT conditions.[19] Covalent bonding to C_{60}^+ is difficult because it is necessary to distort the C_{60} carbon cage at the C-site of bond formation with the substituent so as to achieve the required sp^3 hybridization. Electron transfer with the neutral molecules investigated is endothermic because of the low electron recombination energy of C_{60}^+, RE(C_{60}^+) = 7.64 ± 0.02 eV. The ionization potentials for the neutral reagents all exceed 9.24 eV.[14] $C_{20}H_{10}^+$ (RE = 7.70 ± 0.01 eV) was also found to be unreactive toward all the molecules investigated, $k_{obs} < 10^{-11}$ cm^3 $molecule^{-1}$ s^{-1}.

Under our SIFT conditions, Fe^+ did not react with N_2, D_2, CH_4, CO_2, H_2O, CO, or O_2, $k_{obs} < 10^{-13}$ $cm^3$$molecule^{-1}$ s^{-1}, again in agreement with previous results obtained in our laboratory.[20,21] Addition was observed with SO_2, C_2H_4, C_2H_2, NH_3, and C_6D_6 with effective bimolecular rate coefficients ranging from 8.1×10^{-12} (with SO_2) to 9×10^{-10} (with C_6D_6) cm^3 $molecule^{-1}$ s^{-1}. We have not previously reported the reaction of Fe^+ with SO_2, but the results with C_2H_4, C_2H_2, NH_3, and C_6D_6 agree with our previous measurements.[10,21] A bimolecular reaction involving oxygen atom abstraction and occurring with a rate coefficient of 3.2×10^{-11} cm^3 $molecule^{-1}$ s^{-1} was identified with N_2O, again in agreement with our previous studies.[20] Electron transfer was not observed with any of these molecules because the ionization energy of Fe (IE = 7.9024 ± 0.0001 eV) is too low.

$C_{60}Fe^+$ and $C_{20}H_{10}Fe^+$ reacted with all the neutrals investigated with rate coefficients in the range 6.3×10^{-12}–8.6×10^{-10} cm^3 $molecule^{-1}$ s^{-1}. These correspond to rate enhancements of up to *5 orders of magnitude* when compared with the bare metal ion reactions and nonreactions, as well as the nonreactions of C_{60}^+ or $C_{20}H_{10}^+$ (see Table 1).

We have observed such rate enhancements previously for Fe^+ attached to C_2H_2, *c*-C_5H_5, C_6H_6, and C_{60} in reactions with N_2O and CO when compared with results for the bare metal ion.[8] We have also observed that the ligation of Mg^+ with *c*-C_5H_5

(14) Lias, S. G.; Bartmess, J. E.; Liebman, J. F.; Holmes, J. L.; Levin, R. D.; Mallard, W. G. Ion Energetics Data. In *NIST Chemistry WebBook*; NIST Standard Reference Database No. 69; Mallard, W. G., Linstrom, P. J., Eds.; National Institute of Standards and Technology: Gaithersburg, MD, February 2000 (http://webbook.nist.gov).

(15) Lichtenberger, D. L.; Rempe, M. E.; Gogosha, S. B. *Chem. Phys. Lett.* **1992**, *198*, 454.

(16) Becker, H.; Javahery, G.; Petrie, S.; Cheng, P.; Schwarz, H.; Scott, L. T.; Bohme, D. K. *J. Am. Chem. Soc.* **1993**, *115*, 11636−11637.

(17) Huang, Y.; Freiser, B. S. *J. Am. Chem. Soc.* **1991**, *113*, 8186−8187.

(18) Nakajima, A.; Nagao, S.; Takeda, H.; Kurikawa, T.; Kaja, K. *J. Chem. Phys.* **1997**, *107* (16), 6491−6494.

(19) Bohme, D. K. *Int. Rev. Phys. Chem.* **1994**, *13* (2), 163−185.

(20) Baranov, V.; Javahery, G.; Hopkinson, A. C.; Bohme, D. K. *J. Am. Chem. Soc.* **1995**, *117*, 12801−12809.

(21) Baranov, V.; Becker, H.; Bohme, D. K. *J. Phys. Chem. A* **1997**, *101*, 5137−5147.

Table 2. Summary of Measured Rate Coefficients (k_{obs} in cm^3 molecule^{-1} s^{-1}) and Observed Product Ions for Reactions of Fe^+, $C_{60}Fe^+$, and $C_{20}H_{10}Fe^+$ with Ligand Molecules L Occurring in He at 0.35 Torr and 298 K

L	FeL_n^+	k_{obs}	$C_{60}FeL_n^+$	k_{obs}	$C_{20}H_{10}FeL_n^+$	k_{obs}
D_2	−	$<10^{-13}$	$C_{60}FeD_2^+$	$>6.3 \times 10^{-12}$	$C_{20}H_{10}FeD_2^+$	$>1.6 \times 10^{-11}$
N_2	−	$<10^{-14}$	$C_{60}FeN_2^+$	2.6×10^{-10}	$C_{20}H_{10}FeN_2^+$	1.5×10^{-10}
CO_2	−	$<10^{-15}$	$C_{60}FeCO_2^+$	3.5×10^{-10}	$C_{20}H_{10}FeCO_2^+$	$>5.4 \times 10^{-11}$
CH_4	$FeCH_4^+$	$<5 \times 10^{-14}$	$C_{60}FeCH_4^+$	4.3×10^{-10}	$C_{20}H_{10}FeCH_4^+$	$>1.3 \times 10^{-10}$
			$C_{60}Fe(CH_4)_2^+$	2.9×10^{-12}	$C_{20}H_{10}Fe(CH_4)_2^+$	1×10^{-12}
SO_2	$FeSO_2^+$	8.1×10^{-12}	$C_{60}FeSO_2^+$	6.6×10^{-10}	$C_{20}H_{10}FeSO_2^+$	7.8×10^{-10}
	$Fe(SO_2)_2^+$	1.4×10^{-9}	$C_{60}Fe(SO_2)_2^+$	9.9×10^{-11}		
	$Fe(SO_2)_3^+$	1.2×10^{-9}				
C_2H_4	$FeC_2H_4^+$	6.1×10^{-11}	$C_{60}FeC_2H_4^+$	6.1×10^{-10}	$C_{20}H_{10}FeC_2H_4^+$	6.4×10^{-10}
	$Fe(C_2H_4)_2^+$	6.3×10^{-10}	$C_{60}Fe(C_2H_4)_2^+$	6.9×10^{-10}		
	$Fe(C_2H_4)_3^+$	8.7×10^{-11}				
	$Fe(C_2H_4)_4^+$	3×10^{-13}				
C_2H_2	$FeC_2H_2^+$	1.6×10^{-11}	$C_{60}FeC_2H_2^+$	4.3×10^{-10}	$C_{20}H_{10}FeC_2H_2^+$	4.7×10^{-10}
	$Fe(C_2H_2)_2^+$	7.7×10^{-10}	$C_{60}Fe(C_2H_2)_2^+$	4.6×10^{-10}		
	$Fe(C_2H_2)_3^+$	7.6×10^{-10}	$C_{60}Fe(C_2H_2)_3^+$	2.1×10^{-13}		
	$Fe(C_2H_2)_4^+$	2×10^{-12}				
	$Fe(C_2H_2)_5^+$	5×10^{-12}				
H_2O	−	$<10^{-13}$	$C_{60}FeH_2O^+$	4.2×10^{-10}	$C_{20}H_{10}FeH_2O^+$	4.3×10^{-10}
			$C_{60}Fe(H_2O)_2^+$	4.2×10^{-10}	$C_{20}H_{10}Fe(H_2O)_2^+$	9.8×10^{-11}
			$C_{60}Fe(H_2O)_3^+$	4.5×10^{-11}		
NH_3	$Fe(NH_3)^+$	1.7×10^{-11}	$C_{60}FeNH_3^+$	7.7×10^{-10}	$C_{20}H_{10}FeNH_3^+$	7.2×10^{-10}
	$Fe(NH_3)_2^+$	1×10^{-9}	$C_{60}Fe(NH_3)_2^+$	1.7×10^{-9}	$C_{20}H_{10}Fe(NH_3)_2^+$	2.8×10^{-10}
	$Fe(NH_3)_3^+$	8.2×10^{-12}	$C_{60}Fe(NH_3)_3^+$	1.3×10^{-9}	$C_{20}H_{10}Fe(NH_3)_3^+$	5.9×10^{-11}
	$Fe(NH_3)_4^+$	$<5 \times 10^{-14}$	$C_{60}Fe(NH_3)_4^+$	6.5×10^{-12}		
CO	−	$<10^{-14}$	$C_{60}FeCO^+$	3.9×10^{-10}	$C_{20}H_{10}FeCO^+$	2.5×10^{-10}
			$C_{60}Fe(CO)_2^+$	4.3×10^{-10}	$C_{20}H_{10}Fe(CO)_2^+$	5.3×10^{-11}
			$C_{60}Fe(CO)_3^+$	1.9×10^{-10}	$C_{20}H_{10}Fe(CO)_3^+$	6.7×10^{-12}
			$C_{60}Fe(CO)_4^+$	9.4×10^{-14}		
C_6D_6	$FeC_6D_6^+$	9×10^{-10}	$C_{60}FeC_6D_6^+$	8.6×10^{-10}	$C_{20}H_{10}FeC_6D_6^+$	8.4×10^{-10}
	$Fe(C_6D_6)_2^+$	7.3×10^{-10}	$Fe(C_6D_6)_2^+$			
N_2O	FeO^+	3.1×10^{-11}	$C_{60}FeO^+$	3.1×10^{-10}	$C_{20}H_{10}FeO^+$	2.7×10^{-10}
	$FeO(N_2O)^+$	1.1×10^{-11}	$C_{60}FeN_2O^+$	2.1×10^{-10}	$C_{20}H_{10}FeN_2O^+$	1.1×10^{-10}
	$FeO(N_2O)_2^+$	1.1×10^{-11}	$C_{60}FeO(N_2O)^+$	5.7×10^{-11}		
	$FeO(N_2O)_3^+$	1.4×10^{-11}				
O_2	−	$<10^{-14}$	C_{60}^+	2.0×10^{-10}	$C_{20}H_{10}FeO_2^+$	2.7×10^{-10}
			$C_{60}FeO_2^+$	3.0×10^{-11}	$C_{20}H_{10}Fe(O_2)_2^+$	9.4×10^{-12}
			$C_{60}Fe(O_2)_2^+$	4.2×10^{-11}		

enhances the reactivity of Mg^+ by more than 3 orders of magnitude with methane and ethane[22] and that the *c*-C_5H_5 ligand dramatically enhances the rate of ligation of ammonia to Fe^+ and Mg^+.[10] We have attributed these enhancements to the influence of the degrees of freedom of the ligand L′ effective in the energy redisposition in the intermediate complex, (ML′$^+$−L)*, that is involved in the ligation reaction 2.[10] A more

$$ML'^+ + L + He \rightarrow ML'^+{-}L + He \qquad (2)$$

complete treatment[23] predicts that the rate coefficient for ligation is also determined by the ligand binding energy since the lifetime of the intermediate depends on both the effective degrees of freedom, *s*, in the intermediate (ML′$^+$−L)* and the attractive well depth, $D(ML^+{-}L)$, in the ligated species produced, as shown in eq 3,

$$\tau = A\{(D + 3RT)/(3RT)\}^{(s-1)} \qquad (3)$$

where *A* is a frequency factor corresponding to the vibration frequency along the reaction coordinate.

C_{60} and corannulene add sufficient degrees of freedom to the transient intermediate formed in the ligation reactions of C_{60}-Fe^+ and $C_{20}H_{10}Fe^+$ to enhance substantially its lifetime and therefore the rate of ligation. Furthermore, ligation of Fe^+ with C_{60} and $C_{20}H_{10}$ is expected to lead to a complex with a stronger bonding electronic structure than that of the bare metal ion, and, therefore, to change $D(ML^+{-}L)$. Fe^+ in the ^{6}D ground state ([Ar]4s^{1}3d^6) has a singly occupied, spatially extended 4s orbital, which contributes to repulsive interactions with incoming ligands. In the FeC_{60}^+ or $FeC_{20}H_{10}^+$ complexes, either the 4s orbital is hybridized (sp or sd), resulting in much smaller orbitals, or the 4s electron is promoted into the 3d orbital, leading to a strongly bonding ^{4}F ([Ar]3d^7) configuration (the difference between the ^{6}D and ^{4}F states of Fe^+ is only 5.8 kcal/mol).[24] As a consequence, repulsive interactions with a second molecule of ligand are less pronounced, the bond distances are shorter, and, therefore, stronger electrostatic binding is obtained. Promotion to the ^{4}F state of Fe^+ also increases the metal-to-ligand dative interaction by increasing the number of 3d electrons available for back-donation into π*-orbitals of the ligand.

We assume that the charge in the $C_{60}Fe^+$ and $C_{20}H_{10}Fe^+$ adduct ions is localized primarily at the metal center *at the moment of reaction* due to the electrostatic interaction with the incoming polarizable/polar ligand. The charge distribution in the isolated $C_{60}Fe^+$ and $C_{20}H_{10}Fe^+$ adduct ions is uncertain. The lower ionization energies of C_{60} and corannulene favor electron transfer from C_{60} or $C_{20}H_{10}$ to Fe^+ within the complex ion, but the differences in ionization energy are small. Also, the picture of a metal cation stabilized by the vicinity of the substantial π cloud of a C_{60} or corannulene molecule is more favorable than that of a neutral metal atom in the presence of a C_{60} or corannulene cation.

Sequential Ligation Kinetics. Table 2 summarizes measured rate coefficients and observed product ions for sequential

(22) Milburn, R. K.; Frash M. V.; Hopkinson, A. C.; Bohme, D. K. *J. Phys. Chem.* **2000**, *104*, 3926−3932.

(23) Good, A. *Trans. Faraday Soc.* **1971**, *67* (588), 3495−3502.

(24) Bauschlicher, C. W.; Langhoff, S. R.; Partridge, H. *Organometallic Ion Chemistry*; Freiser, B. S., Ed.; Kluwer: Dordrecht, 1996; pp 47−87.

reactions of Fe^+, $C_{60}Fe^+$, and $C_{20}H_{10}Fe^+$ with ligand molecules L at 298 K in helium buffer gas at 0.35 Torr.

Reactions and CID Results with D_2, N_2, CO_2, and CH_4. One molecule of each of the above neutral reagents was observed to add to $C_{60}Fe^+$, while Fe^+ was unreactive. The rate coefficients varied from 6.3×10^{-12} cm^3 molecule^{-1} s^{-1} (with D_2) to 4.3×10^{-10} cm^3 molecule^{-1} s^{-1} (with CH_4). A second molecule was observed to add to $C_{60}Fe^+$ only in the case of CH_4, and this occurred with a much lower rate coefficient (Table 2). The metal−corannulene ion reacted in a similar way, by adding one molecule of each ligand with rate coefficients ranging from 1.6×10^{-11} cm^3 molecule^{-1} s^{-1} (with D_2) to 1.5×10^{-10} cm^3 molecule^{-1} s^{-1} (with N_2). A second molecule of CH_4 was observed to add slowly to $C_{20}H_{10}Fe(CH_4)^+$.

An equilibrium analysis of the kinetic data for these ligation reactions shows that the reaction of $C_{60}Fe^+$ with D_2 and the reactions of $C_{20}H_{10}Fe^+$ with D_2, CO_2, and CH_4 achieve equilibrium under SIFT conditions. As a consequence, the rate coefficients determined from the rate of decay of $C_{60}Fe^+$ and $C_{20}H_{10}Fe^+$ should be regarded as lower limits. Equilibrium constants (calculated for a standard pressure of 1 atm) of 2×10^5 for $C_{60}Fe^+$ with D_2 and 1×10^6, 1×10^7, and 2×10^7, respectively, for $C_{20}H_{10}Fe^+$ with D_2, CO_2, and CH_4 have been obtained from our kinetic measurements for these reactions. These correspond to a standard free energy change $\Delta G°$ of −7.3, −8.3, −9.5, and −10 kcal mol^{-1}, respectively. For all the other reactions of $C_{60}Fe^+$ and $C_{20}H_{10}Fe^+$, lower limits have been determined for the equilibrium constants, and these all are higher than 3×10^7. Therefore, $\Delta G° < -10.2$ kcal mol^{-1} for all these reactions.

The ionic adducts obtained with these weak ligands are probably purely electrostatic in nature; all these molecules form weak bonds with $C_{60}Fe^+$ and $C_{20}H_{10}Fe^+$ that are broken easily in the CID experiments. Early thresholds for dissociation have been observed for all these adducts (<13−15 V in Ar for $C_{60}Fe^+$ adducts and <20 V in He for $C_{20}H_{10}Fe^+$ adducts). To increase the center-of-mass collision energy, the CID experiments for the fullerene complexes were performed in argon, while for the corannulene complexes helium was used as target gas. In all cases, the fragment ions obtained were $C_{60}Fe^+$ and $C_{20}H_{10}Fe^+$, respectively, suggesting that $D(Fe^+-C_{60}) > D(C_{60}Fe^+-D_2, N_2, CO_2, \text{or } CH_4)$ and $D(Fe^+-C_{20}H_{10}) > D(C_{20}H_{10}Fe^+-D_2, N_2, CO_2, \text{or } CH_4)$.

Reactions and CID Results with C_2H_2, C_2H_4, and SO_2. Two molecules of C_2H_2, C_2H_4, and SO_2 were observed to add to $C_{60}Fe^+$ with primary rate coefficients of 4.3×10^{-10}, 6.1×10^{-10}, and 6.6×10^{-10} cm^3 molecule^{-1} s^{-1}, respectively. Formation of a 3:1 adduct was observed to occur only with C_2H_2, and it proceeded with a small but measurable rate coefficient. Fe^+ also reacted with all these molecules by adding up to five molecules in the same flow range but with primary rate coefficients at least 1 order of magnitude lower than for the reactions of $C_{60}Fe^+$. We monitored the kinetics for Fe^+ in order to make a direct comparison of the reactivity of the bare metal ion with that of its C_{60} and corannulene adducts, and in all cases we have seen a much steeper decay for the adduct−ion reactions and lower degrees of ligation. Except for the reaction with SO_2, which we have not reported previously, the results obtained for Fe^+ confirm results already published by our research group.[10,20,21]

The argon CIDs of the first adduct of $C_{60}Fe^+$ with C_2H_2, C_2H_4, and SO_2 showed thresholds for dissociation around 54, 50, and 60 V, respectively, indicating a much stronger interaction between $C_{60}Fe^+$ and C_2H_2, C_2H_4, and SO_2 compared with the interactions with the weaker ligands D_2, N_2, CO_2, and CH_4. CID was also observed to remove the C_2H_2, C_2H_4, and SO_2 one by one, in reverse order of their addition, suggesting that these molecules are attached to different coordination sites of Fe^+ and do not undergo intramolecular interactions to form chemically bound cyclic or linear structures. $C_{60}Fe^+$ was not dissociated, indicating that $D(Fe^+-C_{60}) > D(C_{60}Fe^+-C_2H_2, C_2H_4, \text{or } SO_2)$.

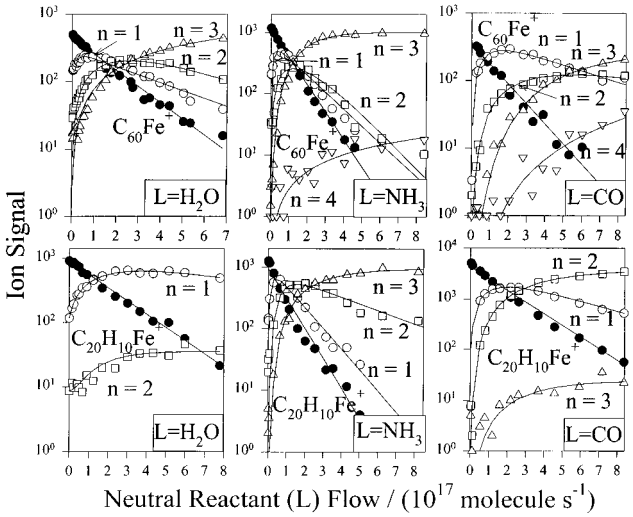

Figure 2. Experimental data for $C_{60}Fe^+$ and $C_{20}H_{10}Fe^+$ reacting with H_2O, NH_3, and CO, where *n* is the number of molecules of ligand attached. The solid lines represent a fit of the experimental data points with the solution of the system of differential equations appropriate for the observed sequential additions. Higher-order adducts were not detected.

The corannulene adduct of Fe^+ reacted with C_2H_2, C_2H_4, and SO_2 also by addition only with rate coefficients comparable to those observed for the C_{60} adduct (4.7×10^{-10}, 6.4×10^{-10}, and 7.8×10^{-10} cm^3 molecule^{-1} s^{-1}, respectively), but only the 1:1 adduct was observed to be formed. CID experiments performed in He showed dissociation thresholds at approximately 65, 60, and 70 V, respectively, proving a stronger interaction than with D_2, N_2, CH_4, and CO_2. Again, the failure to dissociate $C_{20}H_{10}Fe^+$ in all cases shows that $D(Fe^+-C_{20}H_{10}) > D(C_{20}H_{10}Fe^+-C_2H_2, C_2H_4, \text{or } SO_2)$.

Reactions and CID Results with H_2O, NH_3, and CO. Only three water molecules and four ammonia and carbon monoxide molecules were observed to add to $C_{60}Fe^+$ (Figure 2) with rate coefficients of 4.2×10^{-10}, 7.7×10^{-10}, and 3.9×10^{-10} cm^3 molecule^{-1} s^{-1}, respectively. Fe^+ reacted only with NH_3 by adding four molecules.[10b] The argon CIDs of these complexes showed sequential removal of the ligand molecules and high thresholds (50 V for H_2O, 60 V for NH_3, and 50 V for CO) for dissociation of the first adduct, indicating the formation of strong bonds with all these molecules. Again, the Fe^+-C_{60} bond survived at the acceleration voltages that dissociated $C_{60}Fe^+-H_2O$, $C_{60}Fe^+-NH_3$, or $C_{60}Fe^+-CO$, which implies that $D(Fe^+C_{60}) > D(C_{60}Fe^+-H_2O, NH_3, \text{or CO})$.

$C_{20}H_{10}Fe^+$ reacted with H_2O, NH_3, and CO with rate coefficients of 4.3×10^{-10}, 7.2×10^{-10}, and 2.5×10^{-10} cm^3 molecule^{-1} s^{-1}, respectively. Up to two molecules of water and three molecules of NH_3 and CO were observed to attach to the corannulene complex (Figure 2). CIDs of the first adduct in He showed dissociation thresholds higher than 60 V for all three ligands. The observed formation of $C_{20}H_{10}Fe^+$ in each case implies that $D(Fe^+-C_{20}H_{10}) > D(C_{20}H_{10}Fe^+-H_2O, NH_3, \text{or CO})$.

Reactions with C_6D_6. C_6D_6 reacted with Fe^+ by association: two molecules of C_6D_6 were observed to add to Fe^+, while only one molecule of C_6D_6 added to $C_{60}Fe^+$. The adduct $C_{60}FeC_6D_6^+$ reacted further with C_6D_6 by ligand exchange to form $Fe(C_6D_6)_2^+$ according to reactions 4 and 5.

$$C_{60}Fe^+ + C_6D_6 \rightarrow C_{60}Fe(C_6D_6)^+ \quad (4)$$

$$C_{60}Fe(C_6D_6)^+ + C_6D_6 \rightarrow Fe(C_6D_6)_2^+ + C_{60} \quad (5)$$

The unambiguous identification of the product ions of reactions 4 and 5 was made by comparing product ion profiles obtained for Fe^+ reacting with C_6D_6 in the absence and in the presence of C_{60}. This comparison indicates that the $FeC_6D_6^+$ product ion is produced only from the reaction of Fe^+ with C_6D_6 and not from the reaction of $C_{60}Fe^+$ with C_6D_6, while $Fe(C_6D_6)_2^+$ is produced both from the addition of another C_6D_6 molecule to $FeC_6D_6^+$ and from reaction 5.

Freiser and co-workers[6] studied the reaction between C_{60}-Fe^+ and benzene using FT-ICR mass spectrometry; however, they identified $FeC_6H_6^+$ as the only product ion, as in reaction 6. This result disagrees with our result for reaction 4, which

$$C_{60}Fe^+ + C_6H_6 \rightarrow FeC_6H_6^+ + C_{60} \quad (6)$$

suggests that the switching reaction 6 is endothermic at room temperature. In the FT-ICR experiments, $C_{60}Fe^+$ was produced in a multistep process that involved the reaction of Fe^+ generated by laser desorption with pentane to form $Fe(C_nH_{2n})^+$, ($n = 2-5$), followed by ligand exchange reactions with C_{60} vapor and ejection of undesired ions by double-resonance techniques.[2a] It is possible that this production sequence for $C_{60}Fe^+$ leaves this ion sufficiently excited to drive the ligand interchange channel, reaction 6. In the SIFT experiments, the $C_{60}Fe^+$ is more likely to be thermalized as a consequence of the many collisions with He atoms prior to reaction.

In the corannulene experiments, $C_{20}H_{10}Fe^+$ was observed to react with C_6D_6 by forming only the 1:1 adduct, which did not react further.

The ligand exchange reaction observed under our experimental conditions, reaction 5, implies that $D(C_6D_6Fe^+-C_{60}) \leq D(C_6D_6Fe^+-C_6D_6) = 44.7 \pm 3.9$ kcal mol^{-1}.[25] The absence of a similar switching reaction with $(C_{20}H_{10}FeC_6D_6)^+$ suggests a higher bond energy for $Fe^+-C_{20}H_{10}$, allowing us to estimate a lower limit for $D(Fe^+-C_{20}H_{10})$: $D(C_6H_6Fe^+-C_{60}) < D(C_6H_6$-$Fe^+-C_6H_6) = 44.7 \pm 3.9$ kcal mol^{-1} $< D(C_6H_6Fe^+-C_{20}H_{10})$.

Apparent Coordination Numbers Derived from Trends in Reactivity. Aside from the rate enhancement of the primary ligation reaction observed when C_{60} and $C_{20}H_{10}$ are added to the bare Fe^+, our kinetic measurements also reveal that Fe^+, $C_{60}Fe^+$, and $C_{20}H_{10}Fe^+$ add sequentially a different *number* of ligands (see Table 2). The empirical coordination number of Fe^+ already coordinated to either C_{60} or $C_{20}H_{10}$ can be determined from the number of ligands sequentially added with measurable rate coefficients to the point where a significant drop in reactivity occurs. This drop can be associated with coordinative saturation, but only for strong ligands, viz., ligands that are not dissociated thermally or in sampling.

The plots in Figure 3 indicate where this drop in reactivity takes place in the ligation of $C_{60}Fe^+$ and $C_{20}H_{10}Fe^+$. Sometimes the drop is not well defined (as in the ligation of $C_{60}Fe^+$ with C_2H_2, CO, and NH_3). In these latter cases, we take the last drop as a measure of an *apparent* coordination number. This approach

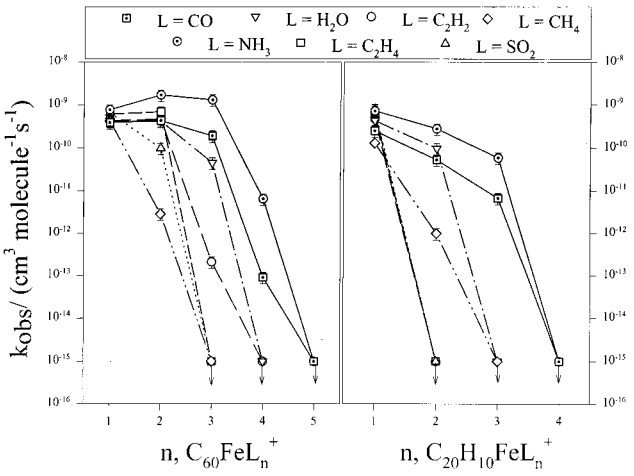

Figure 3. Variation in the rate of sequential ligation (expressed as k_{obs} with the number of ligands, n, for the formation of $C_{60}FeL_n^+$ and $C_{20}H_{10}FeL_n^+$.

provides apparent coordination numbers of 1 for $C_{60}Fe^+$ coordinating with N_2, D_2, CO_2, and C_6D_6, of 2 with CH_4, C_2H_4, and SO_2, of 3 with C_2H_2 and H_2O, and maximum coordination numbers of 4 with CO and NH_3. In a similar way, coordination numbers of 1 were assigned in the ligation of $C_{20}H_{10}Fe^+$ with N_2, D_2, CO_2, C_6D_6, C_2H_2, SO_2, and C_2H_4, while coordination numbers of 2 were assigned with CH_4 and H_2O, and maximum coordination numbers of 3 were assigned with CO and NH_3.

Rationalization of Empirical Coordination Numbers. 1. Location of Fe on the Carbonaceous Surface. There are at least four possible modes of coordination between Fe^+ and the curved C_{60} and corannulene surfaces: η^2, η^4, η^5, and η^6. Under our experimental low-energy conditions, the metal ion attachment to C_{60} is external, but Fe^+ can attach to corannulene from either the convex side (exo) or the concave side (endo), with or without inducing inversion of the bowl. Several experimental and theoretical studies on the external attachment of transition metals to C_{60} have reported that only η^2 coordination is achieved, as opposed to η^5 or η^6 coordination.[3a,c,8,26] Furthermore, it has been suggested that transition metals bind to C_{60} (and to C_{70}) at the C=C bond between two six-membered rings.[3a,26] The curvature of the fullerene surface has been invoked in a possible explanation of the dihapto coordination: on the curved surface the p orbitals are tilted apart, disfavoring η^5 or η^6 overlap with the transition metal orbitals. Also, comparisons with analogous bonding of transition metals to electron-deficient polyalkenes indicate that the carbon−carbon double bonds in C_{60} are ideally disposed to binding in an η^2 fashion, viz., "a combination of both strain and the electron deficiency of the fullerene carbon−carbon double bonds promotes η^2 binding".[3a] The resulting coordination consists of two interdependent components: donation from filled π-orbitals of the double bond to a vacant metal σ-like orbital and back-bonding from a filled metal d orbital to acceptor π^*-antibonding orbitals.[27] The synergic action of these two components (π-donation and back-bonding) avoids the buildup of electron density on the metal and enhances the dihapto bonding.

While the coordination between transition metals and fullerenes has received substantial attention, transition metal coordination to bowl-shaped polyaromatic hydrocarbons (corannulene is the

(25) Meyer, F.; Khan, F. A.; Armentrout, P. B. *J. Am. Chem. Soc.* **1995**, *117*, 9740−9748.

(26) Chen, F.; Singh, D. and Jansen, S. A. *J. Phys. Chem.* **1993**, *97*, 10958−10963.

(27) Dresselhaus, M. S.; Dresselhaus, G.; Eklund. P. C. *Science of Fullerenes and Carbon Nanotubes*; Academis Press: San Diego, 1996; pp 292−328.

smallest and least curved member of this class of compounds) is still relatively unexplored.

Indications so far are that the coordination of corannulene with transition metals may be different from that of C_{60}, even though corannulene is a subunit of C_{60}. Siegel and co-workers[28] have reported hexahapto coordination between corannulene and ruthenium cations in the condensed phase. In their study, the reaction between corannulene and a transition-metal-containing complex, $(C_5Me_5)Ru(NCMe)_3{}^+O_3SCF_3{}^-$, generated (corannulene)-$Ru(C_5Me_5)^+O_3SCF_3{}^-$, in contrast with results reported by Fagan et al.[3a] for a similar reaction with C_{60}, which produced $\{[(C_5Me_5)Ru(NCMe)_2]_3C_{60}\}^{3+}(O_3SCF_3{}^-)_3$. In the latter complex C_{60} is dihapto bonded to three Ru cations and replaces only one acetonitrile unit from the starting metal complex.[3a] The complex obtained by Siegel and co-workers[28] has all three acetonitrile units displaced by corannulene; therefore, hexahapto coordination between corannulene and the transition metal was suggested. However, unlike other known (η^6-arene)$Ru(C_5Me_5)^+O_3SCF_3{}^-$ complexes which are air-stable, the corannulene complex decomposes upon exposure to air.

The difference observed in the coordination with corannulene and C_{60} can be explained, at least in part, by the reduced curvature of corannulene, as compared with that of C_{60}. A π-orbital axis vector (POAV) analysis applied on C_{60} and corannulene[29] showed that the p π-orbitals are tilted by 11.6° on the C_{60} surface and only by 8.7° on the convex side of corannulene. This could favor a better orbital overlap for the η^5 or η^6 coordination of the transition metal to the curved PAH surface. Since the p orbitals are tilted apart (exo) on the convex face of corannulene, they are, correspondingly, tilted toward each other (endo) on the concave face, which could favor endohedral coordination of the transition metal. However, for the metal−corannulene complex obtained by Siegel and co-workers, the exo form of the complex was calculated to be more stable than the endo form at the restricted Hartree−Fock (RHF) SCF level of theory.[28]

We have previously discussed the mode of coordination in $C_{60}Fe^+$.[8] No complexes of Fe^+ with corannulene have been reported, and it is expected that Fe^+ will bind in a different manner than Ru^+, considering that the metal ions have different sizes, which affects orbital overlap with corannulene. Also, the ground-state electronic configuration of Ru^+ ($4d^7$) can contribute to a different bonding interaction with corannulene.

2. Site of Ligation. Where do the ligands attach to $C_{60}Fe^+$ and $C_{20}H_{10}Fe^+$: on the carbonaceous surface or on the Fe substituent? The observation of the failure of $C_{60}{}^+$ and $C_{20}H_{10}{}^+$ to attach the ligands investigated suggests that the carbonaceous surfaces in the Fe adducts are relatively inert (even if they carried the total positive charge). Therefore, we can conclude that the coordination proceeds at the metal center. Indeed, this is where the charge is expected to localize as a consequence of the electrostatic interaction with the incoming polar and/or polarizable ligand.

There are two other observations that support the contention that ligation proceeds at the metal center in $C_{60}Fe^+$ and $C_{20}H_{10}$-Fe^+. In those cases where ligation also is observed with Fe^+, ligation of $C_{60}Fe^+$ or $C_{20}H_{10}Fe^+$ stops at an extent of ligation from one to four ligands less than with Fe^+. Also, we note that the rate of ligation of Fe^+ with the second ligand is similar to the rate of ligation of $C_{60}Fe^+$ or $C_{20}H_{10}Fe^+$ (see Table 2). This implies that C_{60} and $C_{20}H_{10}$ themselves behave as ligands (in the sense that they have paid the promotion energy upon binding to Fe^+) and also suggests that ligation of $C_{60}Fe^+$ and $C_{20}H_{10}$-Fe^+ occurs at the metal center.

Table 3. Known Sequential Bond Energies to Fe^+ (in kcal mol^{-1}) for the Ligands Used in This Work

ligand, L	Fe^+-L	LFe^+-L	L_2Fe^+-L	L_3Fe^+-L	L_4Fe^+-L	ref
H_2	10.8 ± 0.6	15.7 ± 0.7	7.5 ± 0.4	8.6 ± 0.4	2.2 ± 0.3	30
N_2	13.4 ± 1.1					31
CO_2	13.0 ± 1.3					31
	17					32
CH_4	13.7 ± 0.8	23.3 ± 1	23.6 ± 1.4	17.6 ± 1.4		33
C_2H_4	34.7 ± 1.4					34
C_2H_2	28					35
H_2O	33.4	38.5	14.9	11.5		36
NH_3	44.0 ± 2.9	54.3 ± 2.6	16.5 ± 3.6	10.5 ± 1.7		37
CO	37.0	37.0	18.1	22.5	19.2	38
C_6D_6	49.6 ± 2.3	44.7 ± 3.9				25

3. Coordination to $C_{60}Fe^+$. The apparent coordination numbers derived in this study for $C_{60}Fe^+$ can be rationalized in terms of differences expected in the nature and strength of the ligand−metal bonding, although steric effects may also operate. Comparisons with the coordination properties of bare Fe^+ also provide useful insight. Known bond energies for the sequential ligation of Fe^+ with the neutral molecules investigated in this study are presented in Table 3. Both experimental and theoretical values have been cited.

The highest apparent coordination numbers for $C_{60}Fe^+$ (4) were achieved with CO and NH_3. CID experiments showed high thresholds for the dissociation of the first adduct with both CO and NH_3, suggesting strong interactions. Table 3 shows that, after C_6H_6, CO and NH_3 have the highest first binding energies with Fe^+. If C_{60} behaves as a ligand like CO or NH_3, it is reasonable to expect that sequential binding energies to $C_{60}Fe^+$ will be comparable with known sequential bond energies of these ligands once removed (see Table 3). On this basis, we can expect all of the ligation energies in the $C_{60}Fe(CO)_n{}^+$ and $C_{60}Fe(NH_3)_n{}^+$ ions that were observed also to be relatively high (see Table 3), >10 kcal mol^{-1}, and this is born out by the argon CID measurements (see, for example, Figure 4). The helium CID measurements showed higher onsets for dissociation.

Carbon monoxide and ammonia are both strong ligands, and both can contribute two electrons in the bonding with Fe^+ in $C_{60}Fe^+$. The interaction with CO can be described as synergic σ-donation from the ligand to the metal ion and back-donation from the metal into the CO π*-antibonding orbitals. NH_3 should form electrostatic σ-adducts with $C_{60}Fe^+$ by donating its lone pair to the metal center. Thus, coordinative saturation of C_{60}-Fe^+ will be achieved with four molecules of CO (or NH_3) if C_{60} donates two electrons and the metal ion contributes seven electrons to generate a 17-electron species, just as is observed. Proposed structures for these species are presented in Figure 5. This interpretation is supported by the observed stability of

(28) Seiders, T. J.; Baldridge, K. K.; O'Connor, J. M.; Siegel, J. S. *J. Am. Chem. Soc.* **1997**, *119*, 4781−4782.
(29) Haddon, R. C. *J. Am. Chem. Soc.* **1990**, *112*, 3385−3389.
(30) Bushnell, J. E.; Kemper, P. R.; Bowers, M. T. *J. Phys. Chem.* **1995**, *99*, 15602−15607.
(31) Dieterle, H.; Harvey, J. N.; Heinemann, C.; Schwarz, J.; Scroder, D.; Schwarz, H. *Chem. Phys. Lett.* **1997**, *277*, 399−405.
(32) Sodupe, M.; Branchadell, V.; Rosi, M.; Bauschlicher, C. W. *J. Phys. Chem. A* **1997**, *101*, 7854−7859.
(33) Schulz, R.; Armentrout, P. B. *J. Phys. Chem.* **1993**, *97*, 596−603.
(34) Armentrout, P. B.; Kickel, B. L. In *Organometallic Ion Chemistry*; Freiser, B. S., Ed.; Kluwer: Dordrecht, 1996; pp 1−45.
(35) Sodupe, M.; Bauschlicher, C. W. *J. Phys. Chem.* **1991**, *95*, 8640−8645.
(36) Ricca, A.; Bauschlicher, C. W. *J. Phys. Chem.* **1995**, *99*, 9003−9007.
(37) Walter, D.; Armentrout, P. B. *J. Am. Chem. Soc.* **1998**, *120*, 3176.
(38) Ricca, A.; Bauschlicher, C. W. *J. Phys. Chem.* **1994**, *98*, 12899−12903.

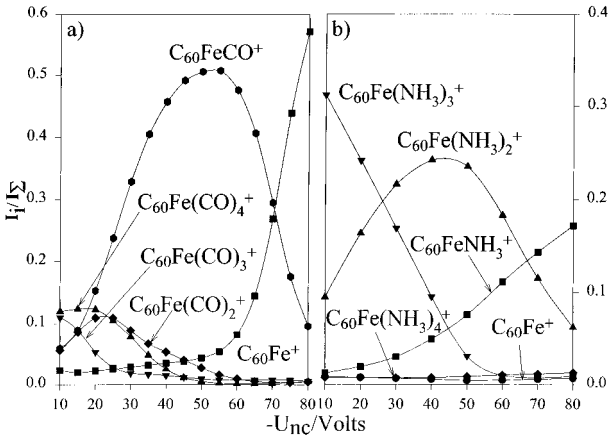

Figure 4. Profiles obtained for the multi-collision-induced dissociation of (a) $C_{60}Fe(CO)_4^+$ in Ar at a CO flow of 1.0×10^{19} molecules s^{-1} and (b) $C_{60}Fe(NH_3)_4^+$ in Ar at a NH_3 flow of 3.8×10^{18} molecules s^{-1}.

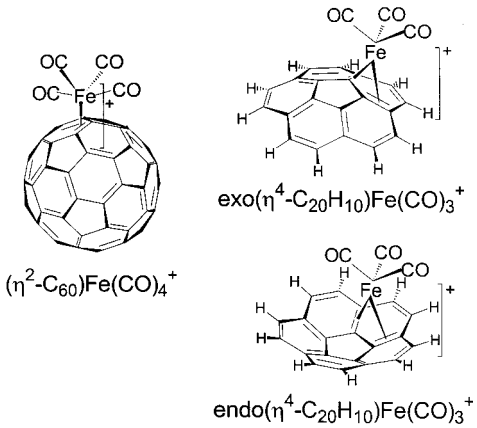

Figure 5. Proposed structures for the terminal product ions observed for the reactions of $C_{60}Fe^+$ and $C_{20}H_{10}Fe^+$ with CO. Not shown is an alternative mode of η^4 binding of $Fe(CO)_3^+$ to corannulene that involves one radial double bond and the rim double bond (both endo and exo).

neutral $C_{60}Fe(CO)_4$, which has been described as an 18-electron complex in which C_{60} acts as a two-electron donor.[3c] Also, previous observations of the gas-phase displacement of CO in $Fe(CO)_5$ by C_{60}^+ are consistent with 2e donation by C_{60} and the formation of a 17e species.[39,40]

$C_{60}Fe^+$ ligated with H_2O, C_2H_2, and C_2H_4 also showed high thresholds for ligand dissociation in CID experiments. These ligands also present high bond energies to Fe^+, as presented in Table 3.

Coordination numbers of 4 are also expected for water (σ-ligand), C_2H_2, C_2H_4, and SO_2 (π-ligands), which may donate two electrons upon ligation, and with water there also exists the possibility of hydrogen bonding in an outer ligation sphere. However, the rate coefficient measurements in Figure 3 indicate lower coordination numbers: 3 for H_2O and C_2H_2 and 2 for C_2H_4 and SO_2. While our CID measurements indicate relatively strong ligation energies for the ligated species that were observed, the trend in these energies indicates a weakening in the ligation energy with increasing ligation. This trend provides an explanation for the lower observed coordination numbers given the dependence of the rate of ligation on ligation energy and possible dissociation of weakly bound ligands.

Similarly, the observed ligation of $C_{60}Fe^+$ with N_2 and CO_2 (π-ligands) as well as D_2 and CH_4 (σ-ligands) does not lead to saturation. Figure 3 indicates apparent coordination numbers of 1 for D_2, N_2, and CO_2 and 2 for CH_4. Our measurements of CID thresholds for these ligands indicate weak interactions.

Binding energies of these ligands to bare Fe^+ are known to be relatively small and this, in part, is due to the zero dipole moments and small polarizabilities of these ligands. It is interesting to note from Table 3 that a sharp drop is indicated for the binding energy of the third hydrogen ligand in $Fe(H_2)_3^+$. If C_{60} behaves as a ligand (as proposed earlier), this drop would predict a similar drop for the binding energy of the second deuterium in $C_{60}(D_2)_2^+$.

Even though N_2 and CO are isoelectronic, differences in the energies of the molecular orbitals of CO and N_2 make N_2 weaker than CO both as a σ-donor and as a π-acceptor.[41] Theory indicates that H_2 binds in a sideways geometry rather than end-on, due to the positive quadrupole moment of H_2 and in order to enhance back-donation of charge from d π-orbitals on the metal to the H_2 σ^*-orbitals.[30]

$C_{60}Fe(C_6H_6)^+$ appears to be coordinatively unsaturated. Since this is a 15-electron species, hexahapto coordination of a second molecule of benzene is not possible. Possible σ-bonding[41] of a second benzene ligand to $C_{60}Fe(C_6H_6)^+$ could not be ruled out since, if weak as is expected, it would be discriminated against in its rate of formation and/or due to experimental conditions.

4. Coordination to $C_{20}H_{10}Fe^+$. Except for C_6D_6 and the weak ligands D_2, N_2, and CO_2 which added once to both $C_{60}Fe^+$ and $C_{20}H_{10}Fe^+$, all other ligands added at least once less to $C_{20}H_{10}Fe^+$ than to $C_{60}Fe^+$. Even with the strong ligands CO and NH_3, only up to three molecules added to the metal−corannulene ion, generating $C_{20}H_{10}Fe(CO)_3^+$ and $C_{20}H_{10}Fe(NH_3)_3^+$. Since the dihapto-coordinated $C_{60}Fe^+$ adds four molecules of CO or NH_3, it can be concluded that corannulene coordinates to Fe^+ in a tetrahapto fashion. Therefore, the smaller curvature of corannulene allows better metal orbital overlap for π-bonding than with C_{60}.

Proposed structures for the carbonyl complexes are presented in Figure 5. The results of our experiments cannot rule whether Fe^+ is exohedrally or endohedrally coordinated to corannulene, but since the energetic cost of inverting corannulene is only 10 kcal/mol,[42a,b] and partial flattening would be even cheaper, it is probably more reasonable to assume that the two structures are interchangeable. According to the proposed tetrahapto coordination of corannulene that involves donation of four electrons, only the CO, NH_3, and C_6D_6 complexes are saturated, 17-electron species. All the other complexes are unsaturated because, presumably, of low reaction rates or experimental discrimination.

A different interpretation of the observed apparent coordination numbers could be given: corannulene binds to Fe^+ in an η^6 fashion, but strong ligands such as CO and NH_3 can easily displace one of the corannulene double bonds to drop the binding to Fe^+ down to η^4. H_2O is too weak a ligand to do this. This will explain why only two molecules of H_2O coordinate to $C_{20}H_{10}Fe^+$ (to give a 17-electron species). In a similar way, C_{60} might be considered weakly η^4 coordinated to Fe^+ most of the time, and strong ligands such as NH_3 and CO can easily displace one of the C_{60} double bonds to drop the binding to the C_{60} down to η^2. This picture would explain why H_2O stops with

(39) Jiao, Q.; Huang, Y.; Lee, S. A.; Gord, J. R.; Freiser, B. S. *J. Am. Chem. Soc.* **1992**, *114*, 2276−2727.

(40) Baranov, V.; Bohme, D. K. *Int. J. Mass Spectrom. Ion Processes* **1997**, *165/166*, 249−255.

(41) Cotton, F. A.; Wilkinson, G. *Advanced Inorganic Chemistry*; John Wiley & Sons: New York, 1980; pp 1049−1182.

(42) (a) Scott, L.; Hashemi, M. M.; Bratcher, M. S. *J. Am. Chem. Soc.* **1992**, *114*, 1920−1921. (b) Biedermann, P. U.; Pogodin, S.; Agranat, I. *J. Org. Chem.* **1999**, *64*, 3655−3662.

three waters on the iron in the $C_{60}Fe^+$ complex. There is no evidence for η^4 coordination of C_{60} coming from condensed phase or from theoretical studies, but η^6 coordination has been observed for corannulene in the ruthenium complex obtained by Siegel and co-workers.[28]

Oxidation Reaction Kinetics. Reactions of $C_{60}Fe^+$ or $C_{20}H_{10}Fe^+$ with oxygen-containing molecules such as H_2O, CO_2, SO_2, and CO did not lead to oxidation by O atom transfer, probably because of the high O atom affinities (OA) of H_2 = 117.4 kcal mol^{-1}, CO = 127.3 kcal mol^{-1}, SO = 131.7 kcal mol^{-1}, C = 257.3 kcal mol^{-1}.[43a,b] Nothing is known about the O atom affinities of $C_{60}Fe^+$ or $C_{20}H_{10}Fe^+$, but the failure to observe O atom transfer with these potential oxygen donors could provide upper limits for OA($C_{60}Fe^+$) and OA($C_{20}H_{10}Fe^+$) of 117.4 (OA(H_2)) or 127.3 kcal mol^{-1} OA(CO)) if exothermicity alone were the criterion for the occurrence of O atom transfer. However, the upper limit of 117.4 kcal mol^{-1} derived from the absence of O atom transfer from water may be problematic since this reaction requires breaking of two O−H bonds and so might have an activation barrier. We have found previously[20] that exothermicity is a valid criterion for O atom transfer to bare Fe^+, and it will be seen next that N_2O, which is a very favorable O atom donor, OA(N_2) = 40.0 kcal mol^{-1},[43b] readily transfers an O atom to $C_{60}Fe^+$ or $C_{20}H_{10}Fe^+$. On the other hand, O_2, a less favorable O atom donor, OA(O) = 119.2 kcal mol^{-1},[43b] simply adds rather than donating an O atom.

Reactions with N_2O. Oxygen atom transfer was indeed identified as an important reaction channel in the reactions of $C_{60}Fe^+$ and $C_{20}H_{10}Fe^+$ with N_2O, but it was observed to compete with the direct addition of N_2O. Branching ratios for O transfer were determined to be 0.60 ± 0.02 for $C_{60}Fe^+$ and 0.70 ± 0.02 for $C_{20}H_{10}Fe^+$. The observation of O atom transfer provides a lower limit for the oxygen affinities of $C_{60}Fe^+$ and $C_{20}H_{10}Fe^+$ of 40.0 kcal mol^{-1}.

One N_2O molecule also was observed to add to $C_{60}FeO^+$, $k = 5.7 \times 10^{-11}$ cm^3 molecule^{-1} s^{-1}, but not to $C_{20}H_{10}FeO^+$, and this is consistent with the lower coordination number observed in this study for $C_{20}H_{10}Fe^+$.

We should compare the rates of oxidation of $C_{60}Fe^+$ and $C_{20}H_{10}Fe^+$ with N_2O to that of the bare metal cation in the absence of a carbonaceous surface. When account is taken of the branching ratio for O atom transfer, the rates of O atom transfer with $C_{60}Fe^+$ and $C_{20}H_{10}Fe^+$ both are found to be 1 order of magnitude higher than the O atom transfer rate for the reaction between Fe^+ and N_2O (see Table 2). Thus, the formation of FeO^+ may be regarded to be "catalyzed" by the presence of either a C_{60} or $C_{20}H_{10}$ carbonaceous surface.

Reactions with O_2. $C_{60}Fe^+$ reacted with O_2 mainly by metal atom transfer, generating C_{60}^+ (reaction 7a). A minor O_2 association channel (reaction 7b) with a branching ratio of (0.13 ± 0.02),

$$C_{60}Fe^+ + O_2 \rightarrow C_{60}^+ + FeO_2 \quad (7a)$$

$$\rightarrow C_{60}FeO_2^+ \quad (7b)$$

followed by a second addition to produce $C_{60}Fe(O_2)_2^+$, also was observed. Available thermodynamics indicates that the neutral product of reaction 7a is FeO_2 and not Fe + O_2 or FeO + O. Recent DFT calculations[44a] indicate three possible stable isomers of FeO_2. These are, in order of increasing stability (where the energy relative to Fe + O_2 is given in parentheses): a bent "superoxo" addition product, FeOO ($\Delta E = -17$ kcal mol^{-1}), a cyclic peroxo adduct Fe(O_2) ($\Delta E = -27$ kcal mol^{-1}), and an oxidative insertion product, bent OFeO ($\Delta E = -64$ kcal mol^{-1}). Linear O−Fe−O and Fe−O−O isomers are higher in energy than Fe + O_2 and therefore thermodynamically unstable.[44b] Formation of FeO + O would require an additional 21 kcal mol^{-1}.[44b] Reaction 7a with Fe + O_2 as neutral products can be calculated to be endothermic by 36.9 ± 7 kcal mol^{-1} from the bracketed value of 44 ± 7 kcal mol^{-1} for $D(Fe^+-C_{60})$[6] and the ionization energies of Fe (7.9024 ± 0.0001 eV) and C_{60} (7.64 ± 0.02 eV). Thus, only the formation of the insertion product OFeO is exothermic in reaction 7a, $\Delta H^0_{298} = -27.1 \pm 7$ kcal mol^{-1}.

A possible reaction pathway for $C_{60}Fe^+$ reacting with O_2 by Fe^+ transfer (reaction 8) was not observed. Theoretical studies[45]

$$C_{60}Fe^+ + O_2 \rightarrow FeO_2^+ + C_{60} \quad (8)$$

have shown that Fe^+ and triplet oxygen molecule can form a side-on peroxo complex, $Fe(O_2)^+$, which easily isomerizes to the high-valent iron oxide, $OFeO^+$. The calculations predict a bond dissociation energy of 24 kcal mol^{-1} for the side-on complex $Fe(O_2)^+$ and of 29 kcal mol^{-1} for the dissociation of $OFeO^+$ into Fe^+ and O_2. The value of 44 ± 7 kcal mol^{-1} for $BDE(Fe^+-C_{60})$[6] indicates that the formation of both of these forms of FeO_2^+ from reaction 8 is endothermic.

The $C_{60}FeO_2^+$ produced in reaction 7b reacted further to add a second O_2 molecule to form $C_{60}Fe(O_2)_2^+$. We note here that bare Fe^+ ions do not add O_2 under SIFT conditions, and this we have ascribed to a short lifetime of the triatomic intermediate complex due to the small number of internal degrees of freedom.[20] The structure of the $C_{60}Fe(O_2)_n^+$ (n = 1, 2) adducts is uncertain, although side-on addition to form a peroxo complex may be preferred for each of the additions, at least initially, on the basis of the computed interaction between bare Fe^+ and O_2.[45] Isomerization to the iron dioxide structure may then ensue. The multi-collision-induced-dissociation experiments indicate a relatively high energy of dissociation but cannot distinguish between loss of an intact O_2 molecule or two O atoms and therefore do not provide further insight into the structures of $C_{60}Fe(O_2)_n^+$ (n = 1, 2).

The reaction between $C_{20}H_{10}Fe^+$ and O_2 exhibited only the addition channel, with two molecules of O_2 attaching sequentially to the metal−corannulene cation. The observation of the sequential addition of only two π-ligands to both $C_{60}Fe^+$ and $C_{20}H_{10}Fe^+$ is unique in the present study. However, differences in the coordination modes are suggested by the kinetic results. Measured rate coefficients for sequential addition presented in Table 2 indicate that ligation of a second molecule of O_2 to $C_{20}H_{10}FeO_2^+$ occurred (more than 1 order of magnitude) more slowly than the addition of the first molecule of O_2 to $C_{20}H_{10}Fe^+$. This is in contrast with the formation of $C_{60}Fe(O_2)_2^+$ from $C_{60}FeO_2^+$ and O_2, which occurred more rapidly than the formation of $C_{60}FeO_2^+$ from $C_{60}Fe^+$ and O_2. Thus, a higher stability is suggested for $C_{60}Fe(O_2)_2^+$, and this is consistent with the measured CIDs.

The absence of the metal atom abstraction channel from the reaction of $C_{20}H_{10}Fe^+$ with O_2 implies that $D(Fe^+-C_{20}H_{10})$ >

(43) (a) *J. Phys. Chem. Ref. Data* **1988**, *17*, Suppl. 1. (b) Wlodek, S.; Bohme, D. K. *J. Chem. Soc., Faraday Trans. 2* **1989**, *85* (10), 1643−1654.

(44) (a) Andrews, L.; Chertihin, G. V.; Ricca, A.; Bauschlicher, C. W. *J. Am. Chem. Soc.* **1996**, *118*, 467−470. (b) Chertihin, G. V.; Saffel, W.; Yustein, J. T.; Andrews, L.; Neurock, M.; Rica, A.; Bauschlicher, C. W. *J. Phys. Chem.* **1996**, *100*, 5261−5273. (c) Helmer, M.; Plane, J. M. C. *J. Chem. Soc., Faraday Trans.* **1994**, *90*, 393−401.

(45) Schroder, D.; Fielder, A.; Schwarz, J.; Schwarz, H. *Inorg. Chem.* **1994**, *33*, 5094−5100.

$D(Fe^+-C_{60})$. This result is consistent with previous expectations, since η^4 coordination is expected to be stronger than η^2 coordination as a result of more efficient back-bonding between the metal ion d orbitals and the antibonding orbitals of the π system.

C_{60}^+ as a Catalyst. Our results suggest a possible role of C_{60}^+ in the catalytic oxidation of iron. The gas-phase reaction of ground-state Fe atoms with O_2 has been shown to proceed only very slowly at room temperature in excess O_2 and N_2 and to exhibit a substantial barrier.[44c] Attachment of Fe atoms to C_{60}^+ according to reaction 10, a reaction that presumably is similar in efficiency to the attachment of Fe^+ to C_{60} observed in the present study, will "activate" the efficient formation of OFeO according to reaction 7a:

$$C_{60}^+ + Fe + He \rightarrow C_{60}Fe^+ + He \quad (10)$$

$$C_{60}Fe^+ + O_2 \rightarrow C_{60}^+ + FeO_2 \quad (7a)$$

Reactions 10 and 7a represent a catalytic chain for the conversion of ground-state Fe atoms and O_2 to iron dioxide. Similar reactions of type (11) leading to the "fixation" of iron are expected to take place between $C_{60}Fe^+$ and other molecules X with high iron metal affinity, $D(Fe-X) > D(Fe^+-C_{60})$.

$$C_{60}Fe^+ + X \rightarrow C_{60}^+ + FeX \quad (11)$$

Conclusions

Rate enhancements of up to 5 orders of magnitude have been observed for the ligation of fullerometallic ions $C_{60}Fe^+$ and $C_{20}H_{10}Fe^+$ with several small molecules when compared with the rates of bare Fe^+ reactions under the same experimental operating conditions (0.35 Torr, helium buffer gas, 298 K). The observed rate enhancements can be accounted for by an increased number of degrees of freedom and electronic effects. Also, indications are that these reactions occur at the metal center, not at the carbon surfaces. Differences in observed product ion distributions for the metal−fullerene and metal−corannulene ions have been used to illustrate differences in the metal ion coordination to the two differently curved carbonaceous surfaces: dihapto for the fullerene coordination vs tetrahapto for the corannulene coordination.

Interesting aspects related to potential catalytic capacities of the carbonaceous surfaces are also revealed. The C_{60} and $C_{20}H_{10}$ surfaces have a catalytic effect on reactions of the iron cation with N_2O and O_2. In the reaction with N_2O, the rate of formation of FeO^+ on the C_{60} or $C_{20}H_{10}$ surfaces is 1 order of magnitude higher than in the absence of these carbonaceous surfaces. In the reaction between $C_{60}Fe^+$ and O_2, an inserted species of neutral FeO_2 is generated in a process in which C_{60} plays a catalytic role.

Acknowledgment. Continued financial support from the Natural Sciences and Engineering Research Council of Canada is greatly appreciated.

Supporting Information Available: Experimental data for reactions of $C_{60}Fe^+$ and $C_{20}H_{10}Fe^+$ with D_2, CO_2, N_2, CH_4, SO_2, C_2H_2, C_2H_4, C_6D_6, N_2O, and O_2 (PDF). This material is available free of charge via the Internet at http://pubs.acs.org.

JA0104857